Flight-Time Identification of Helicopter-Slung Load Frequency Response Characteristics Using CIFER®

Ranjana Sahai
Luigi S. Cicolani

Army/NASA Rotorcraft Division, Ames Research Center, Moffett Field, CA

Mark B. Tischler
Christopher L. Blanken
LTC Christopher C. Sullivan

Army/NASA Rotorcraft Division, Aeroflightdynamics Directorate (AVRDEC)
U.S. Army Aviation and Missile Command, Ames Research Center, Moffett Field, CA

Mei Y. Wei

Western Aeronautical Test Range, Dryden Flight Research Center, Moffett Field, CA

Yat-Sun Ng

Recom Technologies, Inc. , Ames Research Center, Moffett Field, CA

Lawrence E. Pierce

Raytheon ITSS Corp., Ames Research Center, Moffett Field, CA

Abstract

Flight test certification of helicopter-slung load configurations can be time consuming and expensive when quantitative evaluations of the system's handling qualities, stability, and envelope are required. These costs can be significantly reduced by conducting the analysis during the flight test using telemetry data. The analysis is done following the completion of a test point and prior to clearing the aircraft to the next test point. A method for doing this which employs the CIFER® software package for frequency domain analysis of frequency sweep data has been demonstrated in recent slung load flight tests at Ames Research Center. This paper describes the flight-time computational procedure and an efficient graphical user interface designed for the flight-time computations, and presents flight test results. Aircraft frequency responses, handling qualities parameters, stability margins, and load pendulum roots were identified. These computations required about 3 minutes on the 36 MHz workstation used during the flight tests, and this was reduced below 40 seconds on a more modern workstation with 195 MHz processor. The results obtained during the flight test are compared to results from postflight analysis with a more accurate algorithm and with "cleaner" data recorded onboard the aircraft. These comparisons show that the flight-time results provide an accurate assessment of the system dynamic characteristics.

Acronyms

CIFER®	Comprehensive Identification from FrEquency Responses
CONEX	CONtainer EXpress
FFT	Fast Fourier Transform
GUI	Graphical User Interface
PCM	Pulse Code Modulated
PIO	Pilot Induced Oscillation
TM	Telemetry
SAS	Stability Augmentation System

Introduction

Helicopter-slung load operations are common in both military and civil contexts. The slung load adds load rigid body modes, sling stretching, and load aerodynamics to the system dynamics, which can degrade system stability and handling qualities, and reduce the operating envelope of the combined system below that of the helicopter alone. Further, the effects of the load on system dynamics vary significantly among the large range of loads, slings, and flight conditions that a utility helicopter will encounter in its operating life. As a result, incidents and accidents in which the dynamics of the system are unknowingly exceeded are common in the history of slung load operations.[1,2] In this context, military helicopters and loads are cleared for slung load operations via flight tests which can be time consuming and expensive. For example, the UH-60L was certified to carry 9000 lb with a new hook using frequency sweep tests[3] at a cost of several million dollars. Twelve test airspeeds and configurations were flown completing one test point at a time, with stops for engineering analysis between test points. More commonly, specific load-helicopter combinations are certified for the multi-service Helicopter External Air Transport (HEAT) manual[4] via qualitative evaluation for flying qualities and airspeed limits without generating quantitative stability data.

One way to reduce the cost and time required to carry out these tests and generate quantitative data more readily is to provide an efficient method for analysis during the flight, so that numerous test points can be evaluated in a single flight. These evaluations are performed following each test point in near real time to clear the aircraft to the next test point. This methodology was implemented at Ames and demonstrated in slung load flight tests in 1997[5,6] and was improved for additional flight tests in 1999.

The parameters of interest for the slung load tests are aircraft handling qualities parameters (bandwidth and phase delay), stability margins (gain and phase margin), and load pendulum roots (damping and natural frequency). A procedure for the identification of these parameters from frequency sweep data was defined using the CIFER® software package. CIFER® is a comprehensive interactive package of utilities for frequency domain analysis previously developed at Ames[7–9] for aeronautical flight test applications. It has been widely applied in the United States to a variety of aircraft.[10]

CIFER® has a Curses-based general-purpose user interface designed to accommodate many types of frequency domain analyses. Although this interface was successfully used during flight tests in 1997, the numerous and repetitive keyboard inputs required were time consuming and error prone in the real-time context. These factors hampered its effectiveness for flight-time analysis. Consequently, a flight-time graphical user interface (GUI) was designed to operate CIFER® efficiently for the flight tests. The GUI eliminates repetitions by defining the computational steps in advance of the flight, and reduces input errors by using point-and-click inputs. Although the flight-time GUI described here is specific to the slung load computational objectives, the methodology is readily tailored to other applications. Using the flight-time GUI, the complete computational procedure for the aircraft and slung load analysis required less than 2 minutes between flight test points using the GUI with a 36 MHz workstation, and was further reduced to 25 seconds with a more modern 195 MHz workstation.

Since the early 80s, flight-time identification has been exploited in several flight test programs of new aircraft configurations.[11–14] Envelope clearance was completed in hours or a single flight instead of days or multiple flights. These programs have used frequency domain analysis of telemetry data to identify structural mode damping trends from turbulence response data,[11] or to identify stability margins from frequency sweep data.[12–14] In addition, an aerodynamic simulation model has been identified using on-board time-domain analysis of data from maneuver sequences designed to exercise all degrees of freedom.[15] Key elements in these applications have been the data acquisition system, modern workstation computers, and reliable analysis software. All of these flight test projects have reported success in reducing program costs and achieving accurate results from the flight-time analysis, ultimately leading to safer operations.

This paper describes the flight-time computational procedure, an efficient graphical user interface implemented for the flight tests, and provides flight test results to illustrate the success of the method. Some parameters of the computational procedure (data rate, number of windows, removal of correlation with off-axis inputs) were selected to reduce computation time compared to the choices that could be made in postflight analysis where accuracy is the sole consideration. The results presented in this paper indicate that the flight-time algorithm is comparable in accuracy to postflight analysis techniques.

Flight Test Setup

The flight tests were conducted at Moffett Field using the Western Aeronautical Test Range telemetry ground station facility, a Dryden Flight Research Center facility resident at Moffett Field. The data acquisition system is shown in Fig. 1. The test configuration was a UH-60A utility helicopter and various test loads, including the 8×6×6 ft CONEX cargo container seen in Fig. 1. The aircraft was instrumented to measure control deflections, air data, and aircraft attitude, angular rates, and accelerations. A portable instrumentation package was also installed on two of the test loads to measure accelerations, angular rates, and heading.

Frequency sweeps were performed by the test pilot over the frequency range of interest for handling qualities analysis from 0.05 to 2 Hz. A sample time history is shown in Fig. 1. Three sweeps were collected at each test airspeed for each control axis and the sweeps were usually of 90–120 seconds duration. Tests were principally done for the longitudinal and lateral axes, as these are the axes affected by the load motions in the frequency range for handling qualities analysis.

Pulse Code Modulated (PCM) data from both aircraft and load were recorded on board for postflight analysis and simultaneously telemetered to the ground station. The data received at the ground station passed through a server-client system[16] to backup recorders, to strip charts for monitoring, and to a workstation for flight-time analysis. These were all located at the ground station, although the client-server system was capable of broadcasting data to remote sites.

The data stream contained the record number and a data valid flag to indicate the start and end times for a record. This allowed numbered records to pass automatically from the real-time system through gating logic to a Sun Sparc 20 workstation for basic data processing and for the identification computations. The workstation processor speed was 36 MHz. Although current workstations can run an order of magnitude faster, this was adequate speed for the current flight-time analysis.

The tests were conducted with three engineers in the control room to communicate with the pilots, record a test log, provide verbal timing to the pilot during frequency sweeps, monitor sweep frequency and ensure a cutoff when pilot inputs reach 2 Hz, and conduct the data analysis. The cutoff at 2 Hz avoids input frequencies near the UH-60’s lowest frequency lightly damped rotor mode between 2 and 3 Hz.

Computational Objectives

The U.S. military has developed handling qualities requirements that the closed loop system must meet to avoid pilot induced oscillation (PIO) tendencies when the pilot exercises control,[17] and stability margin requirements that the Stability Augmentation System (SAS) must meet to avoid potentially destructive resonance with the plant dynamics.[18] The clearance of loads is concerned with evaluating these handling qualities and stability margins for the combined system as well as the stable speed envelope of the load. The parameters to be identified are the handling qualities bandwidth and phase delay, the gain and phase stability margins, and the load pendulum roots. These results are computed from frequency sweep data taken over the frequency range of interest.

The UH-60 handling qualities parameters are computed from the aircraft closed loop attitude response as illustrated in Fig. 2. Bandwidth for rate command control systems, such as the UH-60 system, is the smaller of the two frequencies corresponding to 45 deg phase margin and 6 dB of gain margin from instability, and represents the largest input frequency for which these margins are obtained. The sample case in Fig. 2 shows multiple values of $\omega_{6\,dB}$ owing to the effect of the load on the response, which produces the gain dip seen in the region of the load pendulum frequency. This effect increases in strength with load weight. As seen in Fig. 2, one of the values is below the pendulum frequency and is of unknown significance in predicting handling qualities for slung loads, so both values will be considered in the analysis. Cases can occur in which the phase shift exceeds 135 deg at all frequencies, in which case the bandwidth is taken as zero.

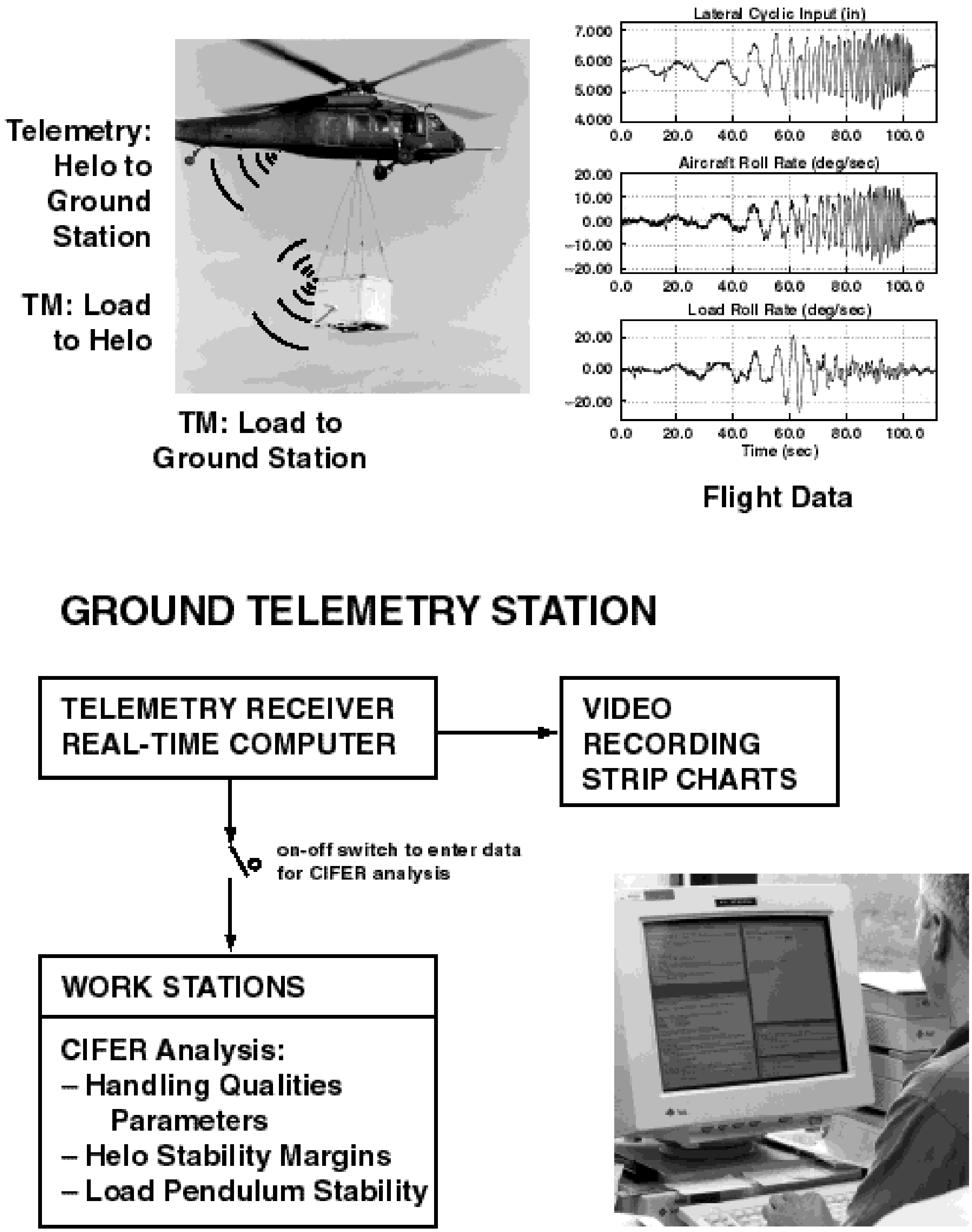

Fig. 1. Data acquisition and flight-time analysis system.

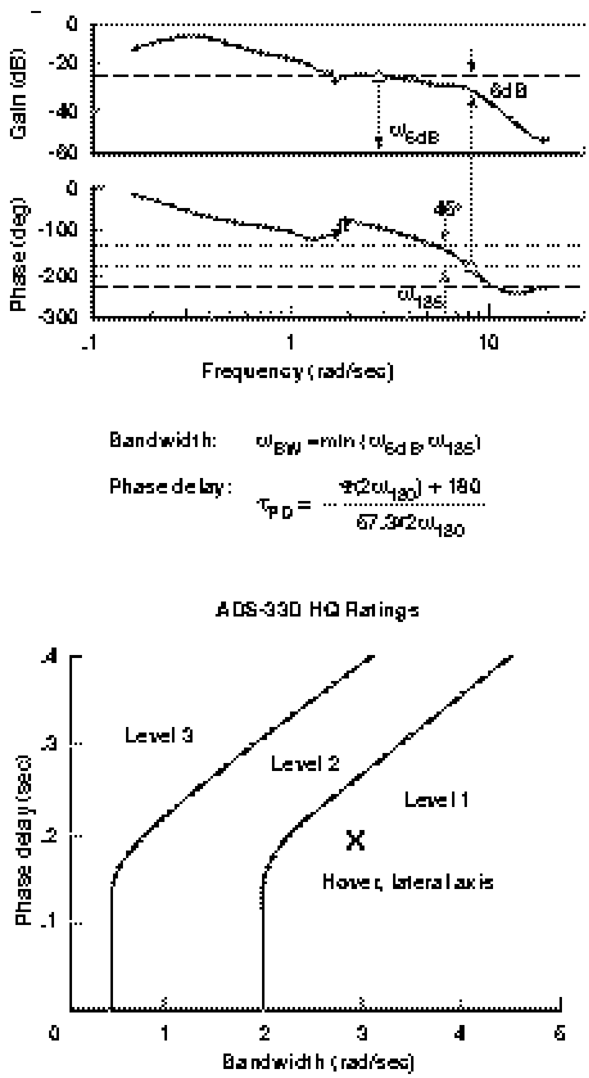

Fig. 2. Identification of handling qualities parameters from closed loop attitude response. Flight condition: hover, lateral axis, 4k lb CONEX.

Phase delay is proportional to the rate at which phase changes at the 180 deg phase shift frequency. The definition is one half the mean slope of the phase curve between the frequency for 180 deg phase shift and twice that, as noted in Fig. 2. Phase delay reflects how fast the pilot-vehicle system stability decreases with frequency. Larger values imply a more rapid loss of stability and result in pilot complaints about PIO tendencies.

The corresponding handling qualities are rated as satisfactory if the combination of bandwidth and phase delay is within the region labeled Level 1 in Fig. 2. Other regions are Level 2 (satisfactory with improvement) and Level 3 (unsatisfactory). The regions shown are established in the U.S. Army's Aeronautical Design Standard, ADS-33,[17] based on flight test and simulation data for scout attack helicopters in non-combat divided attention operations. Corresponding boundaries for utility helicopters and for slung load operations have not yet been defined but are under study by the Army. These ADS-33 boundaries will be used tentatively as the reference requirements herein.

Stability margins are computed from the frequency response of the SAS signal to the inputs to the primary actuators, $\delta_{SAS}/\delta_{ACT}$, or broken loop control response, as illustrated in Fig. 3. These margins are defined for axes with active SAS loops, which are the lateral, longitudinal, and directional axes of the UH-60A. Gain margin is defined at the frequency for 180 deg phase shift, and phase margin is defined at the crossover frequency. Multiple crossovers can occur, as in the figure, in which case phase margin is taken as the smallest margin for crossings in the frequency range of interest. Sometimes the gain curve is below 0 dB at all frequencies (no crossovers), in which case the phase margin is taken as infinite.

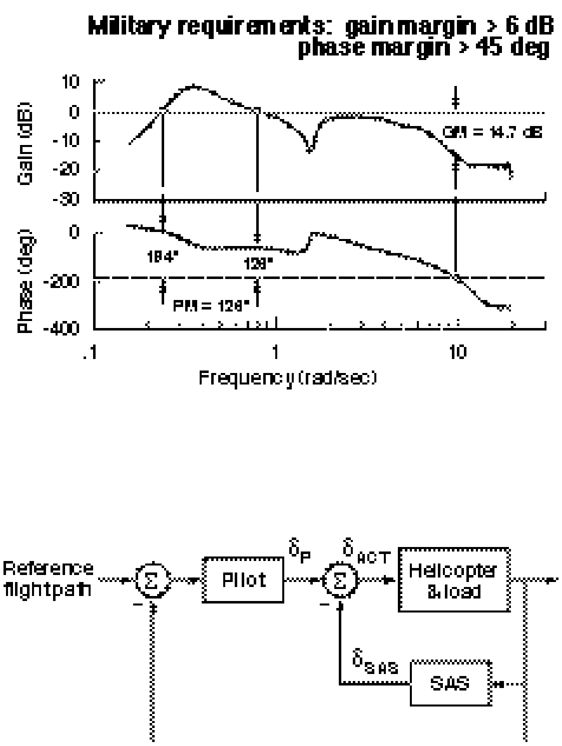

Fig. 3. Identification of stability margins from broken loop control response. Flight condition: hover, lateral axis, 4K lb CONEX.

Military stability margin requirements for production aircraft are 6 dB gain margin and 45 deg phase margin.[18] For some aircraft the critical gain margin occurs at higher frequencies where lightly damped structural modes occur. The UH-60 has a relatively stiff airframe and the critical stability margins occur in the range of interest for handling qualities.

The load adds a number of modes to those of the helicopter alone. Of these, only the pendulum modes interact with the helicopter in the frequency range of interest. For the test system the pendulum frequency was about 1.5 rad/sec. Linear analysis indicates that the pendulum modes at hover are decoupled longitudinal and lateral modes, which are excited by control inputs near the pendulum frequency. Consequently, the load pendulum roots can be identified from the load angular rate response as shown in Fig. 4. The response is seen to have a gain peak and 180 deg phase shift near the pendulum frequency, reflecting the presence of a second-order pole which can be identified by fitting the response in the vicinity of the pendulum frequency. A rule of thumb is to fit the response in the frequency range from 0.5 to 1.5 times the modal frequency.

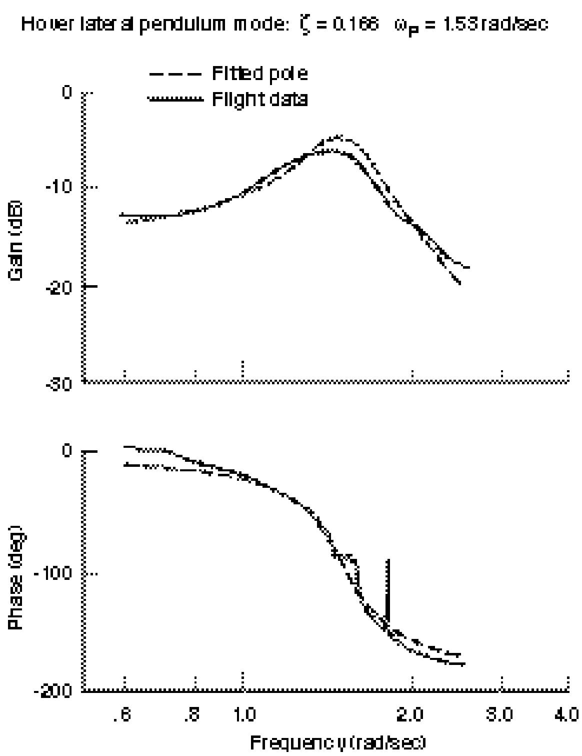

Fig. 4. Identification of load pendulum roots from load angular rate response.

CIFER® Description

In aeronautical use, frequency domain analysis of flight data encompasses a number of objectives, including handling qualities analysis and specification compliance, vibration analysis, and identification of linearized models. The CIFER® software package was developed at Ames to accommodate these objectives[7–9] and is widely used in the United States. It currently runs on VMS and UNIX platforms and a version for NT machines is under development. This package contains various utilities that can be used interactively as shown in Fig. 5 (from Ref. 7). Those of principal interest here are FRESPID, MISOSA, COMPOSITE, NAVFIT, and two analysis utilities.

FRESPID generates frequency responses for input-output pairs from time history data using a flexible form of the fast Fourier transform (the Chirp-Z transform). The record is divided into overlapping time intervals (windows) for computation of the frequency response from averages of the results for the windows. Window size is a selectable parameter that determines the lowest frequency for which the frequency response can be given. Larger windows give better accuracy at lower frequencies while smaller windows improve accuracy at higher frequencies. Accuracy is assessed using the coherence function for the response, which is included in the FRESPID outputs. Coherence measures the linear dependence of the output to the input. This value is always less than one due to nonlinearity of the physical system, secondary inputs, wind turbulence, and signal noise. For reliable identification results, coherence should exceed 0.6 over the frequency range of interest.

MISOSA is used to remove correlation of the output with off-axis control inputs, producing conditioned single-input, single-output responses from multi-input records. Frequency responses can be computed for multiple window sizes and combined to optimize accuracy using COMPOSITE. Up to five window sizes can be combined. Computation of the desired parameters for handling qualities, stability margins, and load pendulum roots utilize the two analysis utilities and NAVFIT. One utility is used to compute the frequency response scalar parameters (crossovers, phase and gain margins, etc.). Derivatives, such as the phase delay, are computed from a coherence-weighted least squares fit over a specified range of data. A second utility is used to carry out frequency response arithmetic (sums, products, integrals, etc.); finally NAVFIT performs optimal fits of specified transfer functions to the frequency responses over specified frequency ranges. The accuracy of a fit is measured by a cost function defined as a weighted sum of the squares of the phase and gain fitting errors. Cost

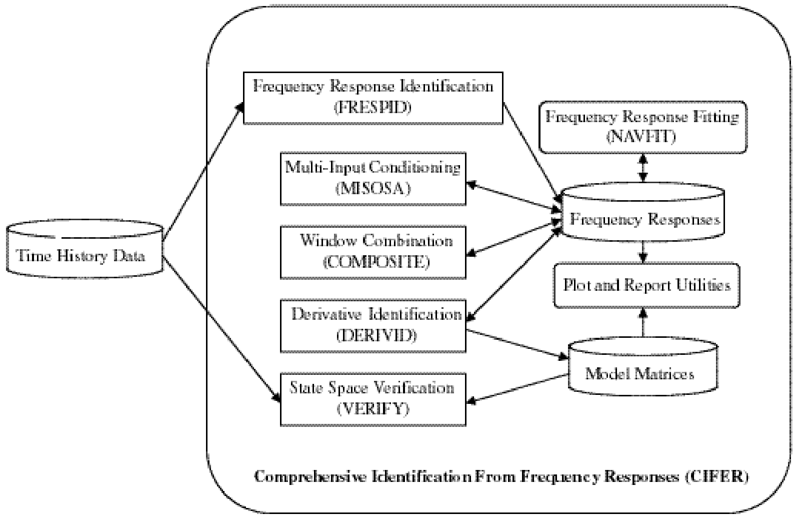

Fig. 5. Major CIFER® utilities and data flow (from Ref. 7).

should be below 100 for the hypothetical fit to be a good approximation of the data.

The earlier flight-time programs reported in Refs. 11–13 have used fast Fourier transform routines (FFT) from IMSL and MATLAB® for the analysis in addition to CIFER®. However, CIFER® provides a comprehensive interactive package for frequency domain analysis, including an advanced Chirp-Z transform for the frequency response computations and the novel ability to optimally combine responses for several window sizes using COMPOSITE.

Computational Procedures

The computational procedure required to carry out the identification of the helicopter-slung load parameters is shown in Fig. 6. First, the available records for the test point are concatenated and the data for the frequency responses are computed for the appropriate input/output pairs and for each window size (FRESPID). Second, correlation with off-axis inputs are removed (MISOSA). Third, the individual frequency responses for the various windows are optimally combined into a single frequency response (COMPOSITE). Last, the desired dynamic parameters for handling qualities, stability margins, and load pendulum roots are computed from the frequency response and plotted (utilities and NAVFIT).

The procedure is characterized by several parameters that affect accuracy and computation time, both of which are of interest for the flight-time procedure. These parameters are the number of records processed, the data rate, the MISOSA computations, and the number of windows.

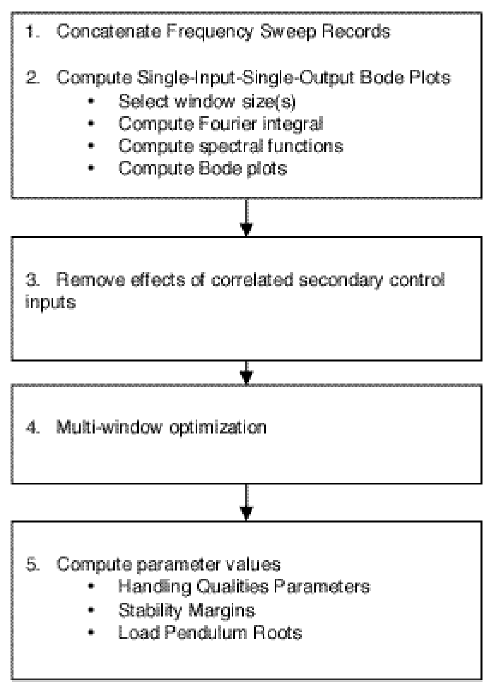

Fig. 6. Identification procedure.

Multiple records, usually three, are taken at each test point to increase the information content and coherence at all frequencies and to average out turbulence effects on the responses to control inputs. In sample cases, a single record produced response plots with complex variations in the range of the 180 deg phase shift frequency and multiple parameter values. The plots converged to smoother curves and a single parameter value as records were added.

The flight data were available at more than 200 Hz. A rule of thumb for adequate data rate for the analysis is to provide data at 16 times the highest frequency of interest. Consistent with this rule, the data were decimated to 50 Hz for the flight-time algorithm and were stored at 100 Hz for postflight processing.

MISOSA removes dependence of the response on off-axis inputs. The pilot attempts to minimize this dependence by using only random, low frequency off-axis inputs to maintain the aircraft centered at the reference flight condition. Consequently, the MISOSA calculations were dropped from the flight-time procedure to obtain a significant reduction in computation time. Tests confirmed that this simplification had very little effect on accuracy.

Five windows at {10, 20, 25, 30, 40} seconds were used in postflight analysis to maximize coherence from the available data. However, computation time increases significantly with the number of windows. For the initial version of the flight-time procedure used in the 1997 flight tests, a single 20-second window was used to provide accurate response down to 0.05 Hz. Good results with adequate accuracy at all test points were obtained. The current flight-time procedure allows a choice of windows and two windows are normally used. Each window adds 30 seconds in computation time for the 36 MHz machine used.

The telemetry data were degraded by dropouts and data spikes that occurred randomly in different signals, or in all signals simultaneously, due to antenna shadowing and multipath effects. FRESPID treats brief random dropouts as high frequency noise. If extended dropouts occurred, the aircraft was reoriented and the record repeated. Degraded data are also reflected in reduced coherence, which is visible in the flight-time frequency response results, so test points with poor coherence could be repeated. The on-board recording used for postflight analysis was free of such dropouts when the recorder operated normally.

Flight-Time Graphical User Interface (GUI)

The standard CIFER® user interface was designed for maximum flexibility of batch processing. It consists of numerous screens, one or more for each utility, with keyboard entry of all items required on each screen. This interface was used in the 1997 flight tests. The CIFER® screens required to generate a frequency response from FRESPID are shown in Fig. 7. The items to specify a case (data file names, variable names, scale factors, the input/output pairs for which frequency responses are to be computed, data rate, number of windows, and window sizes) are contained in eight screens. These are repeated for each of the three frequency responses computed at a test point. These screens can be stored as a single case that serves as a template. A template case for longitudinal and lateral axis analysis was generated prior to the flight test. During the flight test, the appropriate template case was called up and edited for the current test point and the case was then sent for batch processing. Subsequently, parameter computations with the analysis utilities and NAVFIT were performed. These utilities have no template capability and all items required were entered manually. In summary, the execution of the flight-time procedure for a single test point and for a single window analysis with the CIFER® interface required 17 screens and more than 500 keystrokes to enter over 80 items. The same or similar inputs were repeated for each test point.

The standard CIFER® interface, although successfully used in the real-time environment, was obviously inefficient, error prone, and consumed valuable time. Consequently, a more efficient graphical user interface (GUI) was designed for the current flight tests. This flight-time GUI eliminates repetitious inputs, uses point-and-click entries, and minimizes keyboard entries.

The flight-time GUI is a shell program that operates CIFER® for the user. It was constructed using the recently developed scripting languages Tcl/Tk and Expect.[19,20] Tcl (Tool Command Language) is the underlying language used to create the extensions Tk and Expect. Tk (Tool Kit) is used to create the visual part of the graphical interface (the buttons, etc.) and to translate the point-and-click operations into command line instruction while an Expect script operates CIFER®. This flight-time GUI is currently restricted to use on UNIX and NT operating systems since Expect has been developed only for these systems.

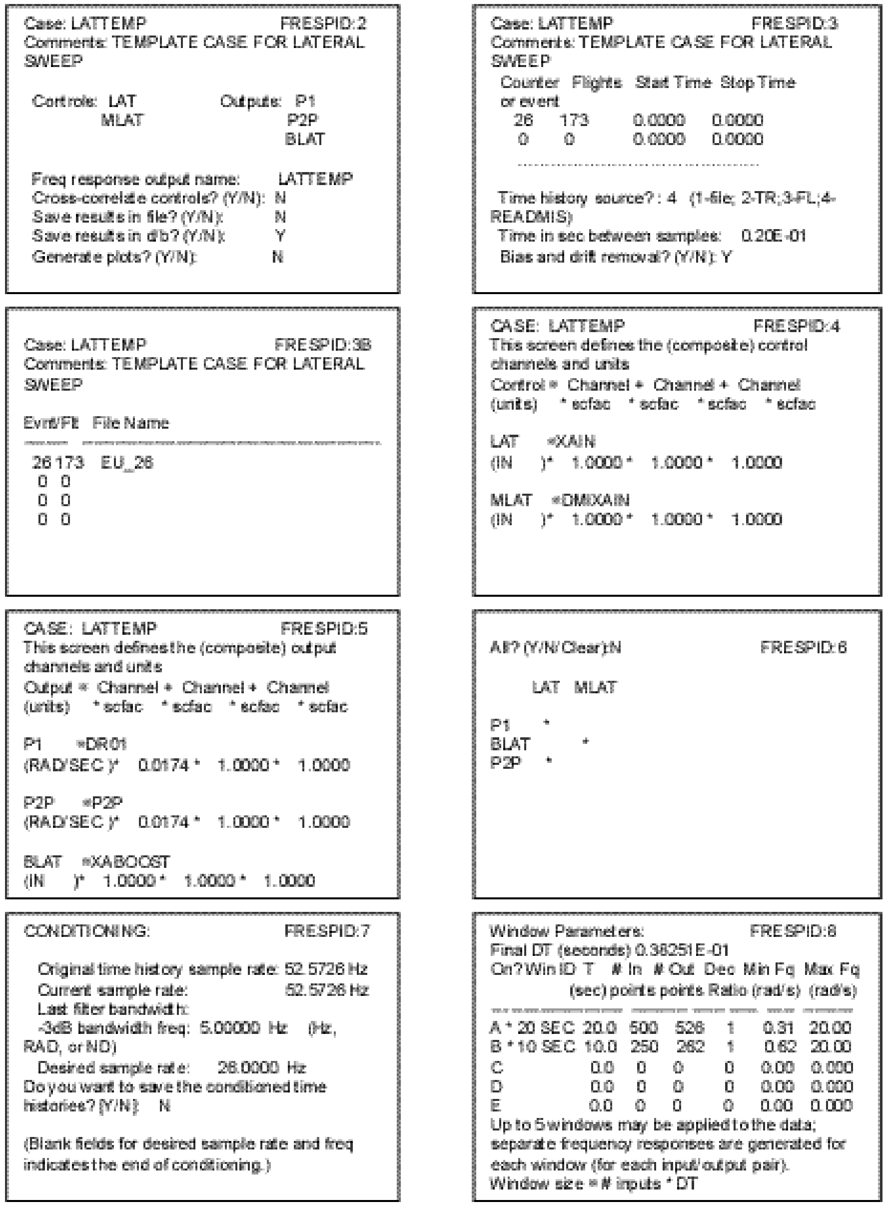

Fig. 7. Excerpts from a template FRESPID case.

The CIFER® flight-time GUI is shown in Fig. 8. It consists of a split screen where the left side contains fields for entering the information required to define each step in the procedure and the buttons to run CIFER® utilities. The right side contains buttons to display the numerical results and plots from the CIFER® analysis. The top left sub-screen is used to edit the FRESPID template of Fig. 7 for the current test point. The lower left sub-screen changes according to the type of computations to be performed (handling qualities, stability margins, or load modes). The example screen shows numerical results and plots for handling qualities parameters. The CIFER® GUI requires entry of only 15 items and 50 point-and-click actions or keystrokes at each test point compared to the 80 items and 500 keystrokes required for the original CIFER® interface.

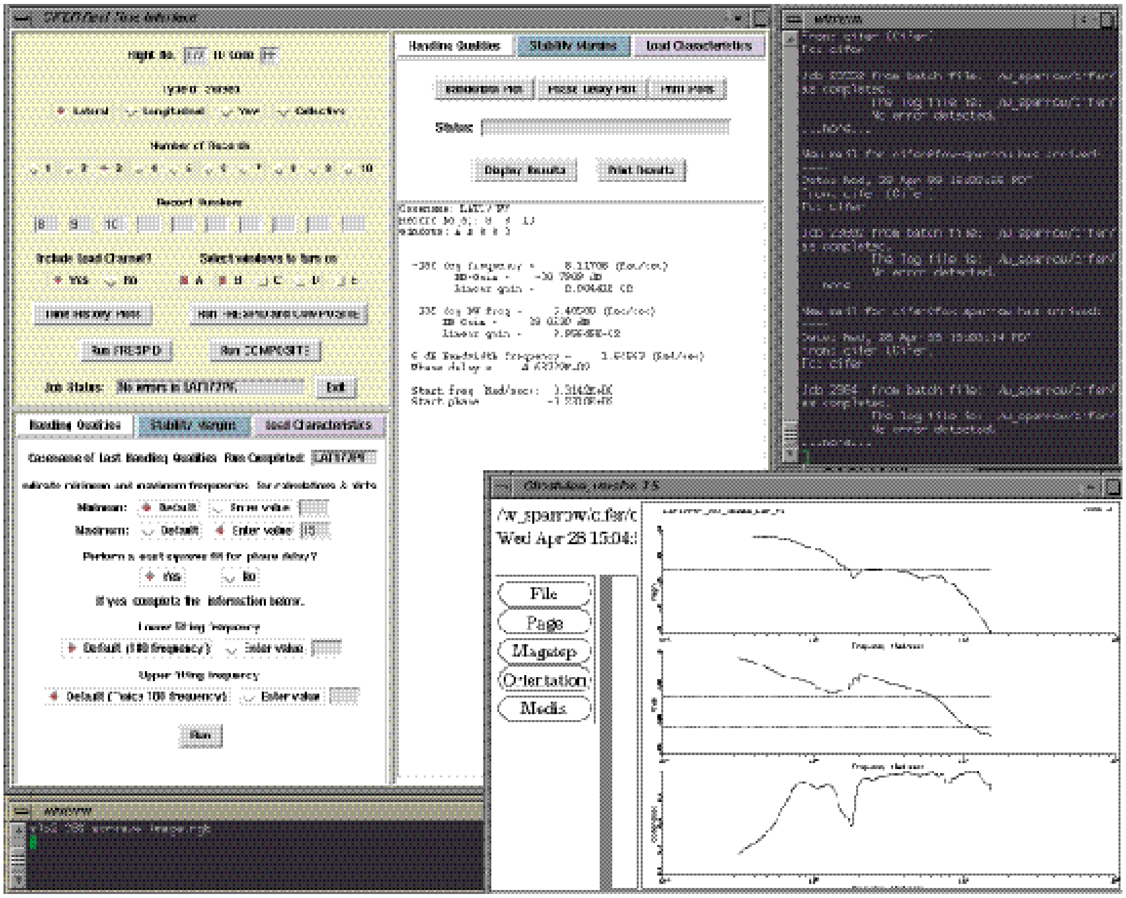

Fig. 8. Graphical User Interface for CIFER®.

Computation time requirements, including analyst entries, are listed in Table 1 for the 36 MHz workstation used for the flight tests. After completion of the flight records, the raw data were processed to decimate the data, convert to engineering units, and compute derived variables (35 seconds). This was followed by FRESPID for 2 windows (80 seconds), COMPOSITE (30 seconds), and parameter computations and display of plots and numerical results (60 seconds). The total time from completion of the flight records to display of the results for a two-window identification of three sets of frequency responses and parameters was under 3.5 minutes. The 1997 flight-time analysis with the CIFER® interface required about 4 minutes. The same single-window procedure with the flight-time GUI requires just over 2 minutes. This saving of time was partly used in the current flight-time analysis work to include the two-window analysis.

During the 3.5-minute period of identification analysis, the pilot carried out other test records such as doublets and trim, but was often available for the next set of frequency sweeps before the completion of the analysis. Further computation time reductions can be obtained using a newer, faster workstation. The procedures above were therefore evaluated on a Silicon Graphics O2 machine with a 195 MHz processor. These times are included in Table 1 and indicate that the flight-time CIFER® analysis can be performed in less than 40 seconds.

The option of adding MISOSA was also considered. However, computation times increase by 85 seconds to compute cross-correlation computations in FRESPID and execute MISOSA. Since the off-axis inputs are usually small and uncorrelated, the addition of the MISOSA option with its large execution time was not considered justified for the 36 MHz workstation used for this flight test.

Table 1. Computation time requirements

Computational component	Time to complete 36 MHz machine, sec	Time to complete 195 MHz machine, sec
Data preprocessing	35	
FRESPID (one window)	65	9
FRESPID (two windows)	80	14
FRESPID (two windows and cross correlation)	125	44
COMPOSITE (two-window case)	30	6
MISOSA (two-window case)	40	4
Handling qualities, stability margins, load roots	60	17

Identification Results

Results are reviewed in this section to demonstrate the effectiveness and accuracy of the flight-time identification. Attention is also given to the differences between flight-time and postflight results and to the causes of these differences, which can be due either to the difference between the flight-time and postflight computational procedures or to the differences between the telemetry data and data recorded on-board.

Results for a sample test point (hover, lateral axis, 4K lb CONEX load) are shown in Fig. 9. Figure 9a shows the telemetry time history data consisting of three sweeps concatenated together. The pilot enters a sinusoidal control with smoothly increasing frequency from 0.05 Hz to 2 Hz. Each record begins and ends with 3 seconds of trim. Control amplitude is reduced at low frequency to avoid excessive attitude excursions, and increases to 1–1.5 inches of stick travel (10–15%) for the remainder of the record. The helicopter roll rate is seen to respond at all frequencies. The attitude response is obtained by integrating this signal rather than using the recorded attitude signal. This is because the signal-to-noise ratio in the rate record at the high end of the frequency range is greater owing to sensor dynamics. The load roll rate responds to inputs principally in the neighborhood of the pendulum frequency and is attenuated at other frequencies. Since the load body axes are in general spinning or crabbed relative to the helicopter body axes, the load body axes angular rate signals are transformed to axes aligned with the helicopter longitudinal and lateral axes for the load pendulum analysis. The transformed roll rate is shown in Fig. 9a. Two additional control signals complete the set of signals required for the identification analysis. A number of wild points are visible, and these are typical of telemetry data.

Figure 9b compares the flight-time and postflight closed loop attitude frequency responses. A further comparison with the one-window flight-time identification is included. The effects of the load appear as a gain dip and phase shift at the pendulum frequency (around 1.5 rad/sec). The flight-time computations with two windows capture these effects accurately while the use of single-window analysis results in some small but visible mismatch at the pendulum frequency. Away from the pendulum frequency the flight-time and postflight results are nearly identical. Differences between the two sets of results occur at frequencies where coherence is reduced, at the pendulum frequency and at frequencies above 10 rad/sec. The loss at the pendulum frequency occurs because the pilot input is absorbed by the load at this frequency. The two-window flight-time analysis maintains coherence very close to that of the postflight analysis, while the one-window flight-time analysis loses more coherence.

The frequency range of coherence above 0.6 (adequate coherence) is greater for the postflight analysis than the flight-time computations. Tests indicate that wild points in the TM data are treated as high frequency noise that characteristically reduces coherence at the high end of the frequency range. The minimum frequency for the results is set by the largest window size, which is 20 seconds (0.05 Hz) and 40 seconds (0.025 Hz) for flight-time and postflight computations, respectively.

The broken loop control responses are compared in Fig. 9c. The load again produces a gain dip and phase shift at the load pendulum frequency. The responses agree closely, but small differences are visible at the pendulum frequency and at the 180 deg phase shift frequency. The latter difference results in a 3 dB gain margin difference

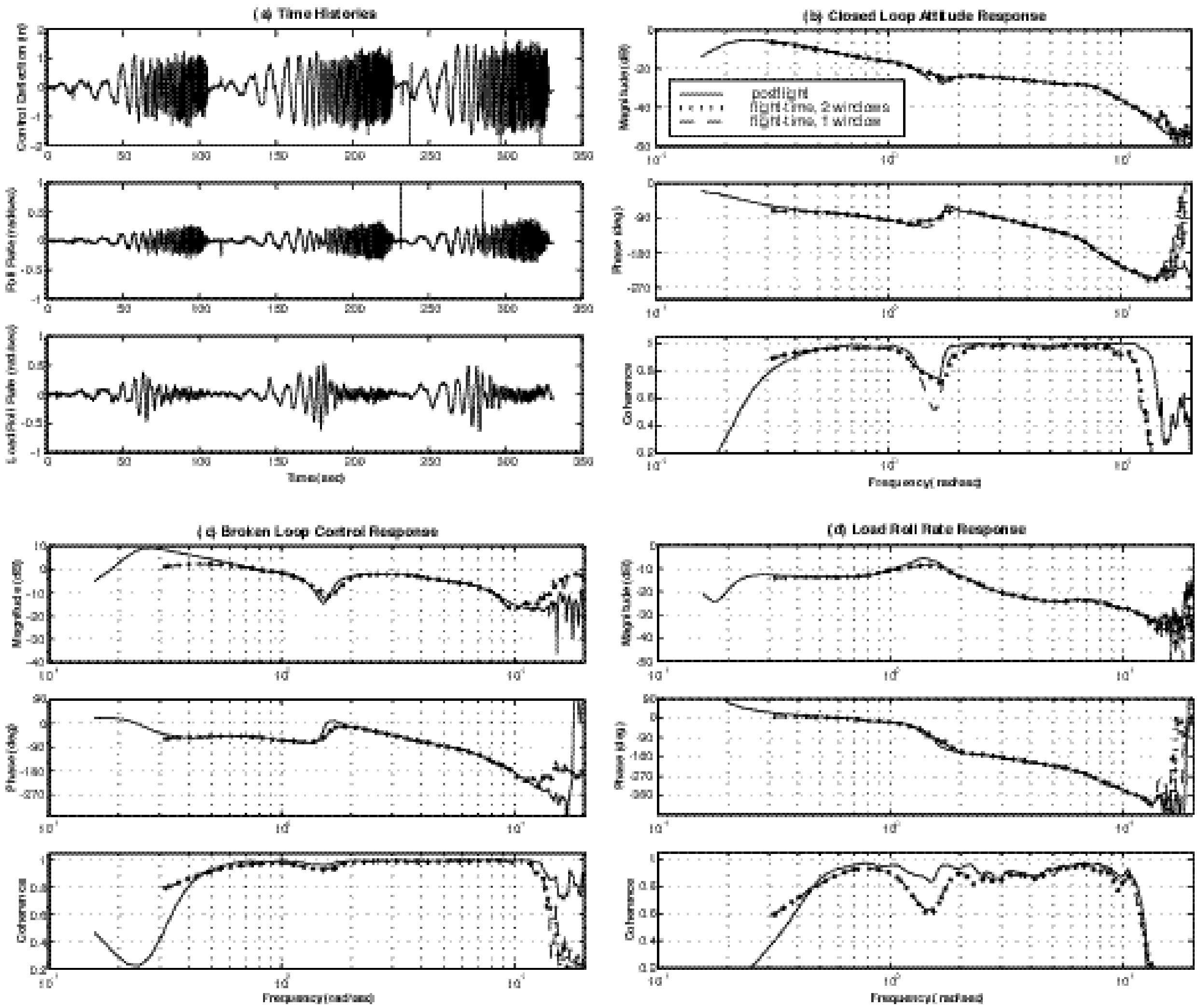

Procedure	Band-width	Phase Delay	Phase Margin	Gain Margin	Pend Damping	Natural Freq
postflight	3.02	.0965	130.5	14.8	.158	1.51
flight-time	2.59	.1178	125.6	17.2	.200	1.60

Fig. 9. Sample case frequency responses: hover, lateral axis, 4K lb CONEX.

between the flight and postflight identifications. There is little difference in accuracy for the one- and two-window analyses, although additional tests on this case indicate that the response differences are due largely to differences in the flight-time and postflight computational procedure.

Load roll rate responses are compared in Fig. 9d. The load responds only at the pendulum frequency with a gain peak at that frequency and a 180 deg phase shift in the region. The comparison shows small differences in both gain and phase near the pendulum frequency where the identification is made. Coherence is reduced in this range, with a greater reduction for the flight-time identification. Tests indicated that these differences were due to the differences in the flight-time and postflight computational procedure and not to differences in the signal quality of the TM and on-board data. The flight-time results with one and two windows are nearly identical, so the added window did not improve the identification for this case. However, useful improvements were obtained with the two-window procedure for many other cases.

Parameter values for the CONEX load at several test speeds are compared in Fig. 10. The handling qualities parameters (Fig. 10a) agree closely in all cases. Stability margins (Fig. 10b) agree closely except for the hover, longitudinal axis gain margin, which differs by 5 dB. Tests indicated this was due to the difference in signal quality between TM and on-board data, which resulted principally in gain curve differences at the 180 deg phase shift frequency. Load pendulum roots (Fig. 10c) show moderate differences in lateral pendulum damping. Adequate coherence was increasingly difficult to obtain for the CONEX load response as airspeed increased, and a credible identification could not be obtained at 50 knots.

Figure 11 illustrates a case in which the wild points and inaccuracies in the TM data have a small effect on the responses but an important effect on the identified parameter values. The sample is hover, lateral axis with the 4K lb block load. A cluster of wild points is seen in the second record of the concatenated time histories (Fig. 11a). The resulting frequency responses (Fig. 11b) show small complex differences in the region of the 180 deg phase shift frequency at 8 rad/sec. The corresponding handling qualities parameter values differ significantly. The flight-time algorithm was rerun using the on-board data and the agreement in both response and parameter values was much closer. This finding demonstrates that the parameter mismatch is due to the difference in the two data sets. A similar comparison of the broken loop response (Fig. 11c) shows even larger flight-time versus postflight differences, particularly in stability margin values. The use of the on-board data with the flight-time algorithm shows a significant improvement in coherence and close agreement in response details at higher frequencies and in parameter values. Some differences remain at and below the pendulum frequency which reflect the difference in algorithms.

A comparison of the control input time histories in Figs. 9a and 11a indicates that the input frequency sweeps in Fig. 11a are not as good; the records are shorter with less time spent at higher frequencies. Nevertheless, the postflight results have adequate coherence for the identification, and the quality of the input is not a factor in this case. Also, the identification analysis is robust with respect to the quality of the input sweep in this case. However, cases have occurred during the tests in which poor input histories result in poor coherence. These are immediately evident as a result of the flight-time analysis and the test point can be repeated.

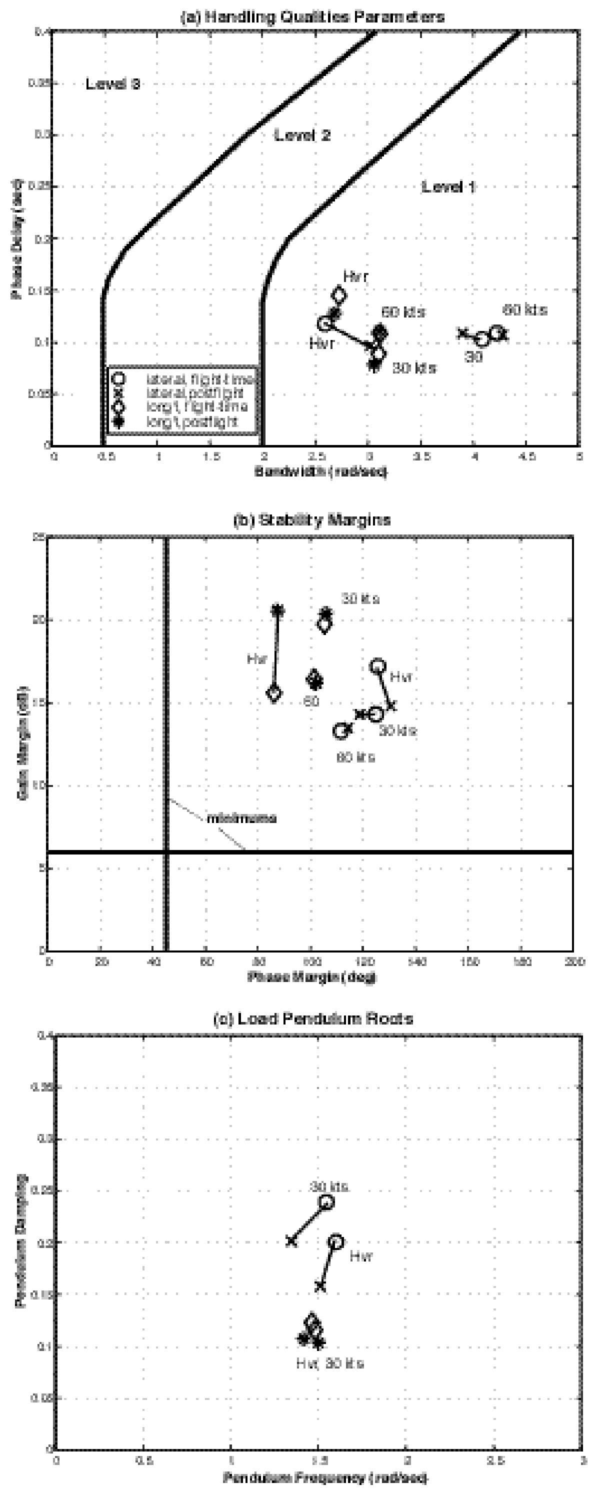

Fig. 10. Comparison of paramegter values: 4K lb CONEX.

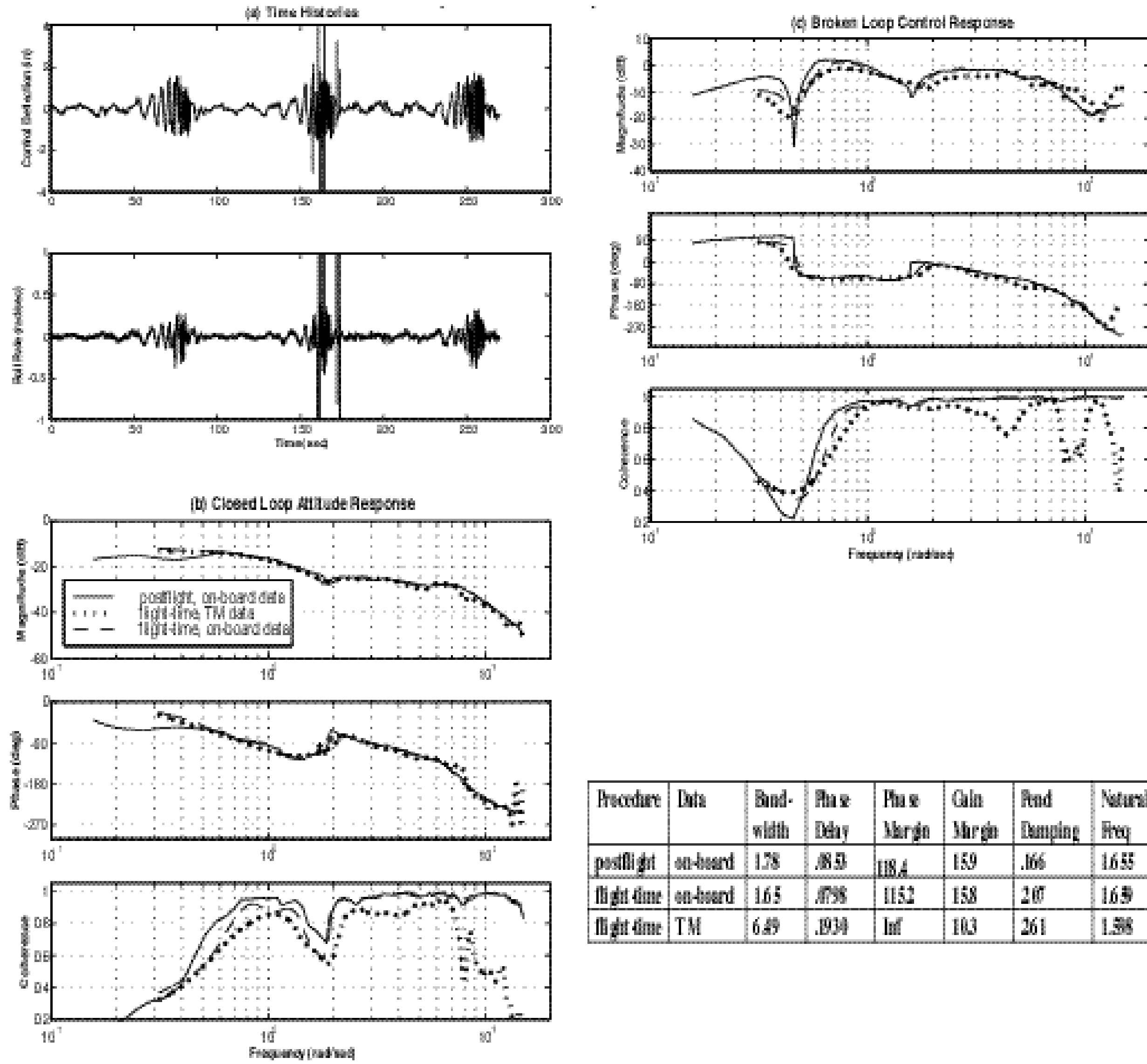

Procedure	Data	Band-width	Phase Delay	Phase Margin	Gain Margin	Pend Damping	Natural Freq
postflight	on-board	1.78	.0853	118.4	15.9	.166	1.655
flight time	on-board	1.65	.0798	115.2	15.8	.207	1.659
flight time	TM	6.49	.1934	Inf	10.3	.261	1.598

Fig. 11. Sample case effects of telemetry data wild points: hover, lateral axis, 4K lb block load.

Figure 12 shows results for the heaviest test load, a 6K lb block, which is about 46% of the helicopter weight. The handling qualities parameter values (Fig. 12a) agree closely. The increased load weight drives the lateral axis handling qualities into the level 2 region. As previously noted, the handling qualities ratings boundaries in the figure are those for scout attack vehicles. Corresponding boundaries for slung loads have not yet been established and the ratings shown here are tentative. In any case, the flight-time identification accurately captured the loss of bandwidth for the lateral axis. Stability margins (Fig. 12b) show good agreement except for lateral axis phase margin at 30 and 50 knots. This occurs because the flight-time response gain is below 0 dB for the whole frequency range, in which case the phase margin is taken as infinite. However, there is only a small difference in the gain curve between the flight-time and postflight analyses. Thus, some parameter values of interest can vary discontinuously with small changes in the frequency responses, particularly phase margin and the 6 dB bandwidth in the present work. This effect is more an artifact of the definitions of the stability and handling qualities measures than a problem of frequency response accuracy. In the sample cases, the analyst recognizes that the difference between phase margin values in excess of 100 deg does not alter the stability assessment.

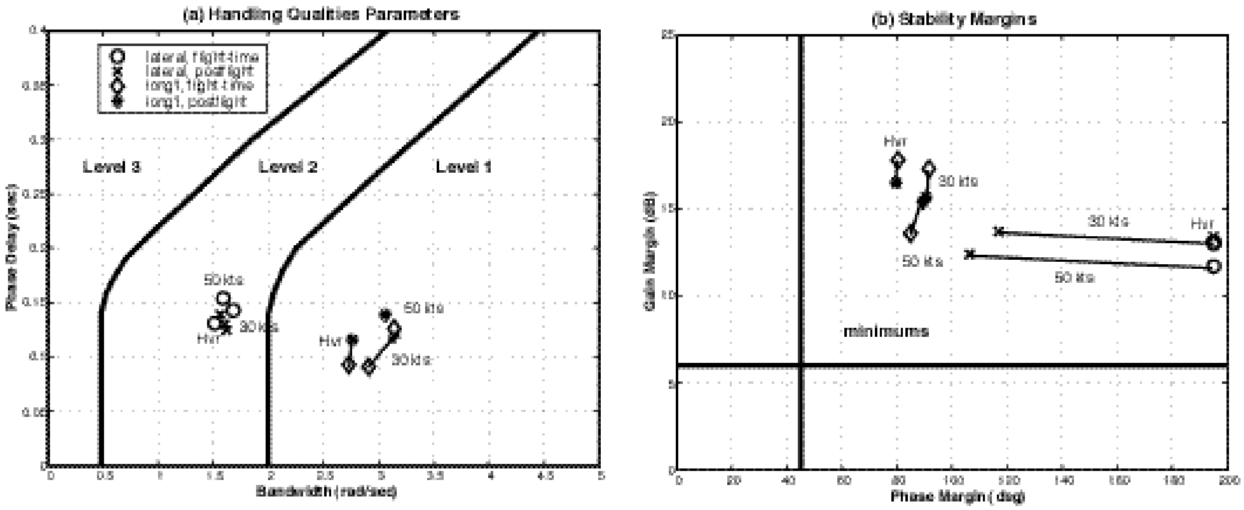

Fig. 12. Comparison of parameter values: 6K lb block load.

The slung load flight test experience reported above indicates several factors underlying the differences between flight-time and postflight analyses. First, signal errors associated with telemetry transmission used during flight-time analysis are not present in the on-board data used for postflight analysis. These telemetry errors effectively limit the accuracy of the flight-time analysis. Telemetry errors, such as dropouts and wild points, were shown to reduce coherence at higher frequencies and introduce small differences in the frequency responses. These small differences in the frequency responses sometimes produce important differences in the parameter values computed from them. Second, differences due to the reduced accuracy of the flight-time computational procedure were noted, but in no case resulted in significant mismatches of the parameter values. Finally, it was also noted that some parameter values were volatile with small differences in the responses. Again, this finding is more related to the definitions of the parameters used in the evaluation than to a problem of identification accuracy. The analyst can account for such parameter sensitivity by reviewing the frequency responses as well as the parameter values.

Conclusions

Flight testing with a flight-time analysis tool applied to the identification of slung load dynamic characteristics leads to the following conclusions:

1. A practical method has been demonstrated for applying CIFER® to identify helicopter-slung load handling qualities and stability during flight tests.

2. A flight-time graphical user interface has been implemented which minimizes the time, effort, and keyboard error probabilities in executing the CIFER® analysis for the near-real-time flight test context.

3. A simplified computational procedure has been shown to achieve good accuracy in computing aircraft handling qualities parameters and stability margins, as well as load pendulum roots.

4. Experience indicates that degraded coherence can occur due to degraded telemetry data or to problems in the execution of the test maneuver. This is evident from the flight-time analysis, which allows the test point to be repeated immediately.

The effectiveness and benefits of the flight-time identification method using CIFER®, which was demonstrated here for slung load clearance testing, is expected to be readily obtained in many other flight test programs.

References

[1]Shaughnessy, J. and Pardue, M., “Helicopter Sling Load Accident/Incident Survey, 1968–1974,” NASA TM X-74007, Mar. 1977.

[2]Key, D., “Analysis of Army Helicopter Pilot Error Mishap Data and the Implications for Handling Qualities,” *European Rotorcraft Forum*, Rome, Sept. 1999.

[3]Lawrence, T., Gerdes, W., and Yakzan, S., “Use of Simulation for Qualification of Helicopter External Loads,” *Proceedings, AHS 50th Annual Forum*, May 1994.

[4]Multiservice Helicopter External Air Transport: Vols. I, II, III, U.S. Army FM-55-450-3,4,5, Feb. 1991.

[5]McCoy, A., “Flight Testing and Real Time System Identification Analysis of a UH-60A Black Hawk Helicopter with an Instrumented External Sling Load,” NASA CR–1998-196710, Apr. 1998.

[6]Cicolani, L., McCoy, A., Tischler, M., Tucker, G., Gatenio, P., and Marmar, D., “Flight-Time Identification of a UH-60A Helicopter and Slung Load,” NASA TM–1998-112231, Apr. 1998.

[7]Tishler, M. and Cauffman, M., “Frequency-Response Method for Rotorcraft ID: Flight Applications to BO-105 Coupled Rotor/Fuselage Dynamics,” *JAHS*, July 1992.

[8]Tischler, M. and Cauffman, M., “Comprehensive ID from Frequency Responses (CIFER®): An Interactive Facility for System ID and Verification. Vols. 1, 2,” NASA CP-10149, USAATCOM TR-94-A-017, Sept. 1994.

[9]Ham, J., Gardner, C., and Tischler, M., “Flight-Testing and Frequency Domain Analysis for Rotorcraft Handling Qualities,” *JAHS*, Apr. 1995.

[10]*Advances in Aircraft Flight Control* (M. B. Tischler, Editor), Taylor and Francis Inc., Bristol, Pa., 1996.

[11]Kehoe, M. W., “AFTI/F16 Aeroservoelastic and Flutter Flight Test Program: Phase I,” NASA TM-86027, Sept. 1985 (restricted distribution).

[12]Bosworth, J., “Flight-Determined Longitudinal Stability Characteristics of the X-29 Aircraft Using Frequency Response Techniques,” NASA TM-4122, 1989.

[13]Balough, D., “Determination of X-36 Stability Margins Using Real-Time Frequency Response Techniques,” *Proceedings, AIAA Atmospheric Flight Mechanics Conference*, Aug. 1998.

[14]Lisoski, D. and Tischler, M. B., “Solar Powered Stratospheric Research Aircraft—Flight Test and System Identification,” *Proceedings, NATO/RTO Symposium on System Identification for Integrated Aircraft Development and Flight Testing*, Madrid, May 1998.

[15]Breeman, J., Kannemans, H., and Laban, M., “In-Flight Model Identification Research Aimed at Developing a Flight Simulator Model,” *Proceedings, NATO/RTO Symposium on System Identification for Integrated Aircraft Development and Flight Testing*, Madrid, May 1998.

[16]Ng, S., Wei, M., Somes, A., Aoyagi, M., and Leung, J., “Real-Time Data Server-Client System for the Near Real-Time Analysis of Ensemble Data,” *Proceedings, International Telemetry Conference*, San Diego, Calif., Oct. 1998.

[17]Handling Qualities Requirements for Military Rotorcraft, U.S. Army Aeronautical Design Standard ADS-33D-PRF, USAATC/AVRDEC, U.S. Army Aviation and Troop Command, St Louis, Mo., May 1996.

[18]General Specification for Flight Control Systems: General Specification for Design, Installation, and Test of Piloted Aircraft, Mil-F-9490D. Dept. of Defense, June 1975.

[19]Welch, B. B., *Practical Programming in Tcl and Tk*, Prentice Hall, Upper Saddle River, N.J., 1995.

[20]Libes, D., *Exploring Expect*, O’Reilly & Associates, Sebastopol, Calif., 1995.